Supplementary Information for

Esophago-Inspired Magnetic-Driven Soft Robot for Directional Transport of Objects

*Shanfei Zhang[a]†, Qi Wang[b]†, Zhuofan Li[b], Yizhuo Xu[a], and Bin Su[a]**

[a] State Key Laboratory of Material Processing and Die & Mould Technology, School of Materials, Science and Engineering, Huazhong University of Science and Technology, Wuhan 430074, Hubei, China

[b] State Key Laboratory of Advanced Electromagnetic Engineering and Technology, School of, Electrical and Electronic Engineering, Huazhong University of Science and Technology, Wuhan 430074, Hubei, China

* To whom correspondence should be addressed: B. Su. (subin@hust.edu.cn)

CONTENT

Movie S4. The hydrogel sphere was transported continuously by “cross” and “straight” shaped soft robots.

Movie S5. MESR successfully transported objects underwater.

Movie S6. MESR successfully transported liquid metal underwater.

Movie S7. 3D-MESR successfully transported objects from various channels.

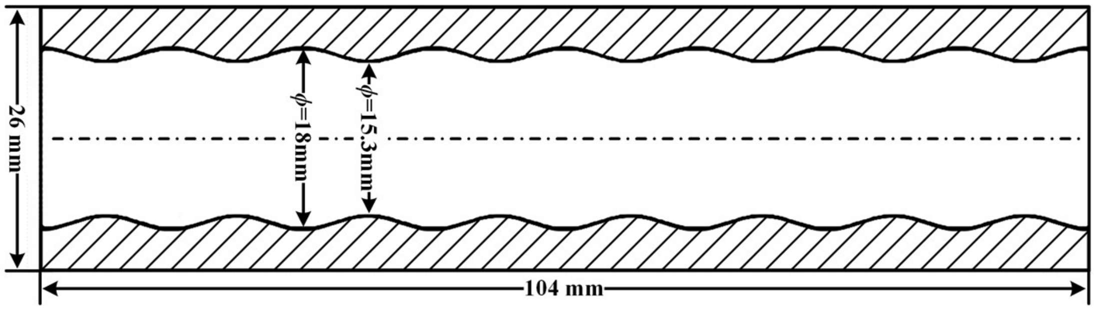

Fig. S1. Profile structure of a mold used to assist in the preparation of MESR.

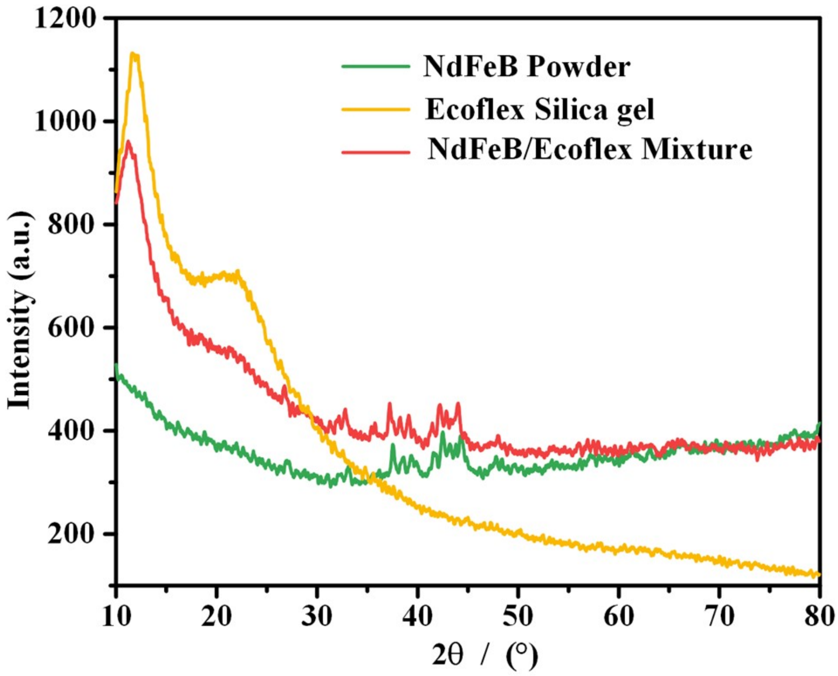

Fig. S2. XRD pattern of Ecoflex silica gel, NdFeB magnetic powder and NdFeB/Ecoflex mixture.

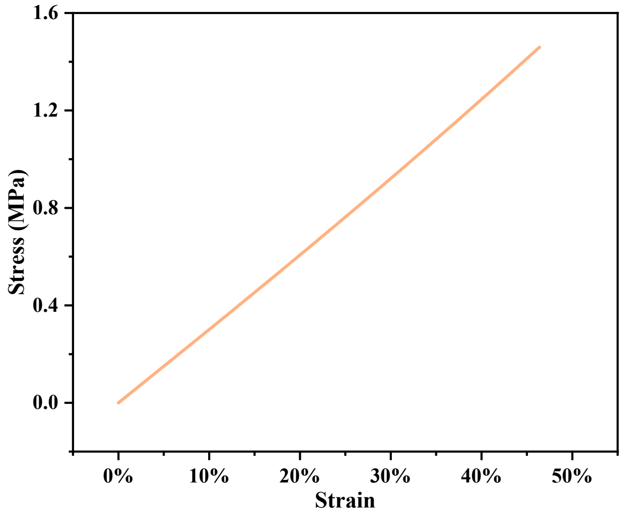

Fig. S3. Stress-strain curve of magnetic composite of MESR.

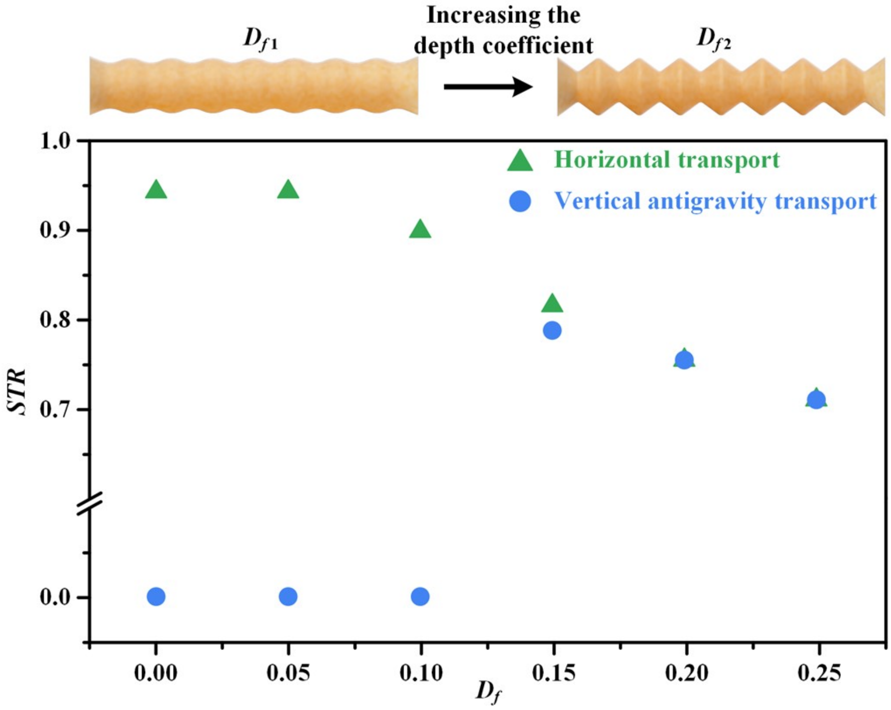

Fig. S4. The influence of wave depth coefficient D_f of MESR on its transport capacity.

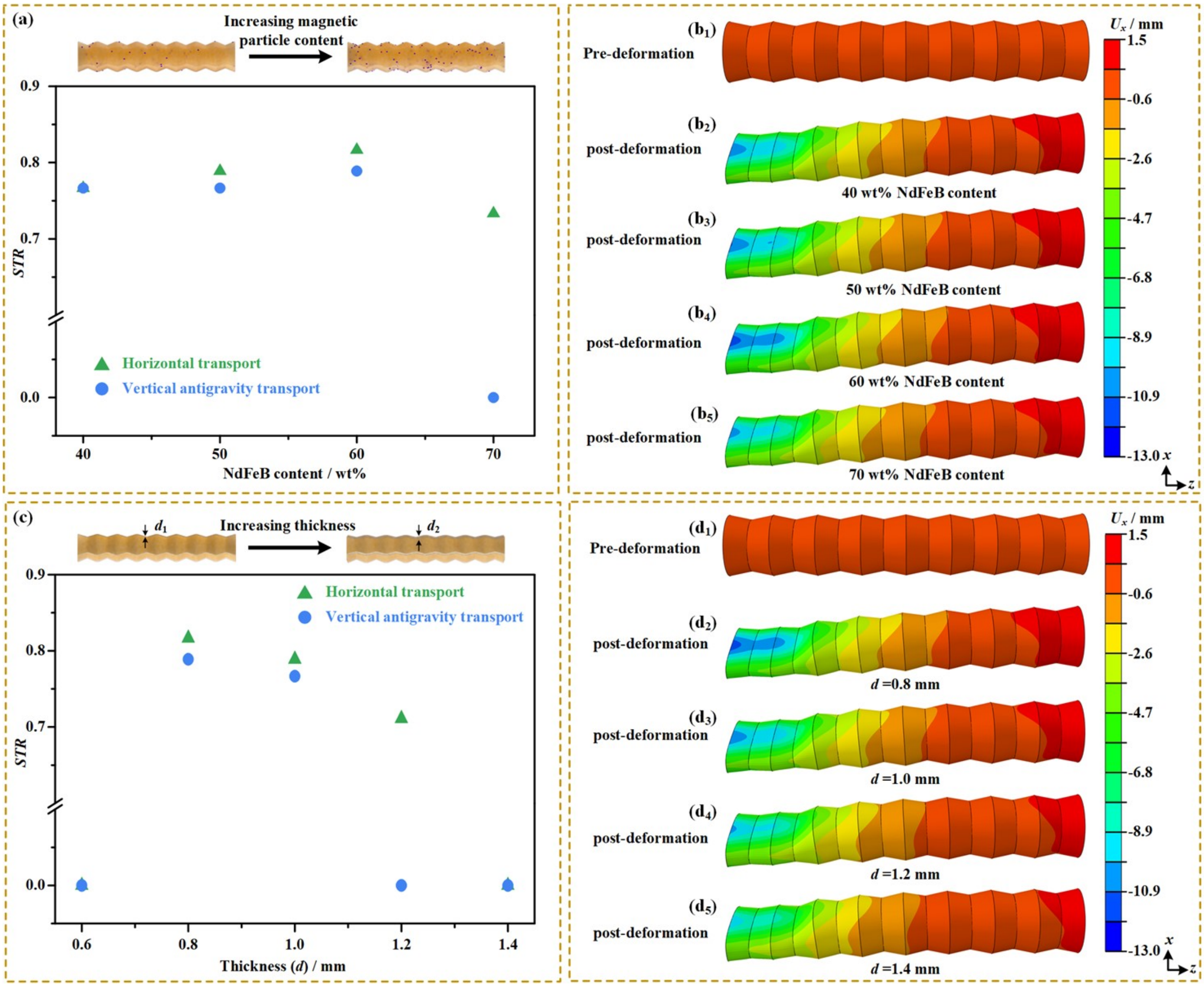

Fig. S5. Effect of NdFeB magnetic particle content and thickness d of MESR on its transport capacity. (a) Effect of NdFeB magnetic particle content and (c) thickness on the transport capacity of MESR. Numerical simulation of the effect of (b_1) - (b_5) NdFeB powder content and (d_1) - (d_5) thickness on the magnetic drive denaturability of MESR.

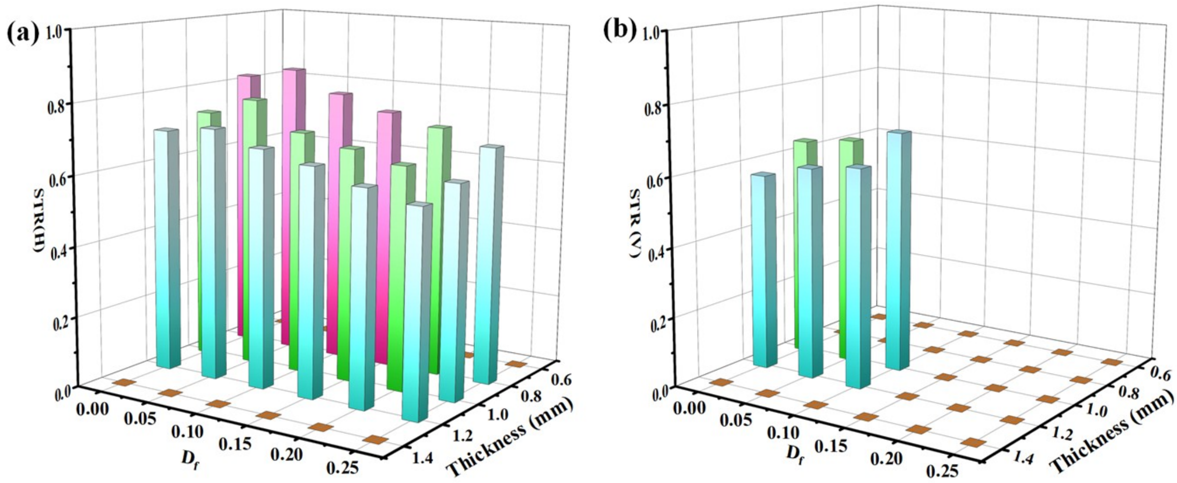

Fig. S6. The effects of three factors on the successful transport rate in vertical direction (STR(H)) and horizontal direction (STR(V)) of MESR were studied by orthogonal experiments. (a) and (b) are the effects of the content of NdFeB and thickness on STR(H) and STR(V), respectively. (c) and (d) are the effects of depth coefficients (D_f) and NdFeB on STR(H) and STR(V), respectively. (e) and (f) are the effects of thickness and depth coefficient (D_f) on STR(H) and STR(V), respectively.

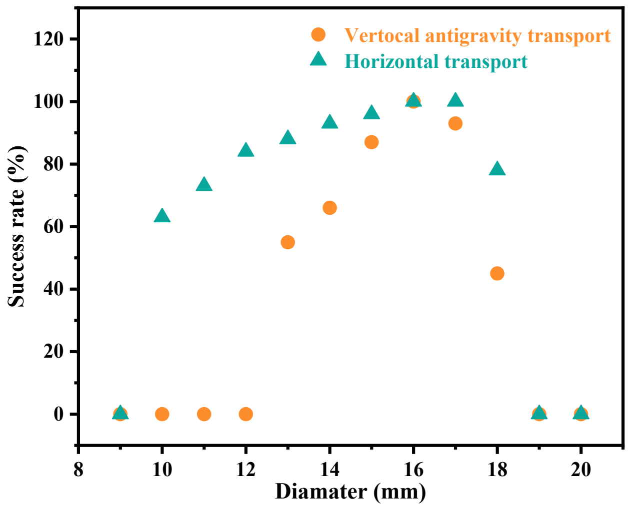

Fig. S7. The success rate of EMSR transport of hydrogel balls of different diameters.

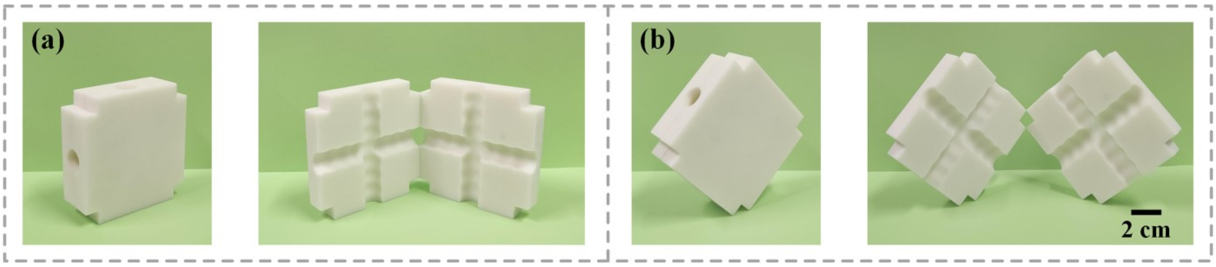

Fig. S8. Optical photos of 3D printing molds used to assist in the preparation of 3D-MESR.

Fig. S9. The machine hand device for controlling the magnet.

Table S1. Mechanical and magnetic parameters of soft composites with different magnetic powder content NdFeB/Ecoflex magnetic response.

NdFeB content（wt %）	Remanent magnetism B_r（T）	Remanent magnetization M_r（kA/m）	Density ρ（g/cm^3）	Shear modulus μ（kPa）	Bulk modulus K（MPa）
40	0.0528	42.02	1.60	31.6	3.16
50	0.0760	60.48	1.84	43.1	4.31
60	0.1075	85.55	2.17	49.7	4.97
70	0.1526	121.44	2.64	103.6	10.36

Note S1. Numerical simulation method.

Abaqus software was used to simulate and study the deformation mechanism and deformation ability optimization of MESR under the action of external magnetic field. The magnetic and mechanical parameters of NdFeB/Ecoflex magnetic response soft composite materials with different magnetic powder content used in numerical simulation were shown in **Table S1**. The remanent magnetic direction of each part of the MESR structure is shown in **Fig. 3c_1-c_2**. In addition, it can also be seen from **Fig. 4** that due to the periodic corrugated structure of MESR, all parts of MESR can shrink and deform under the action of magnetic field. Therefore, taking the magnetic drive deformation of the first chamber of MESR as an example (corresponding to **Fig. 4a_1-a_2**), the numerical simulation study was conducted, and the chambers of the second and subsequent sections of the robot were approximately not subject to the action of magnetic field.

To facilitate the calculation, the NdFeB/Ecoflex magnetic response MESR model was equivalent to a macroscopic homogeneous permanent magnet based on the homogenization equivalent theory. The quantitative equivalent magnetic constitutive relation is:

$$B = \mu_r^{'} \mu_0 H + B_r^{'} \quad \textbf{(S1)}$$

Where $\mu_r^{'}$ is the equivalent relative permeability of the composite with a magnitude of approximately 1, μ_0 is the permeability of the vacuum, and $B_r^{'}$ is the equivalent remanence of the composite.

The saturated magnetized MESR material model has a uniform distribution of residual magnetic moment M_r with constant size and direction. Under the action of the applied magnetic field B^a, the residual magnetic moment M_r will be subjected to the action of the magnetic torque, so as to turn in the same direction as the applied magnetic field B^a. This magnetic moment-turning process will change the stress distribution inside the material and eventually lead to the magnetically driven macroscopic deformation of the material. During the turning of the residual magnetic moment M_r inside the material, the applied magnetic field B^a will do work on the residual magnetic moment M_r, and then change the strain energy density of the material. The change of the strain energy density can be expressed by the formula S2, and the magnetic constitutive relation of the NdFeB/Ecoflex magnetic response composite is shown by the formula S1. Formula S2 can be further written in the form shown in formula S3.

$$W = M_r \cdot B^a \tag{S2}$$

$$W = M_r \cdot B^a = \frac{B_r^{'}}{\mu_0} e_m \cdot B^a \tag{S3}$$

Where e_m is the unit vector of the magnetization direction of the magnetic response soft composite.

Under the assumption of small deformation, the Neo-Hookean constitutive model is used to describe the mechanical properties of NdFeB/Ecoflex magnetic response composites in the absence of an applied magnetic field. The strain energy density function W can be written in the form of the formula S4:

$$W = \frac{\mu}{2}\left(J^{-1.5} I_1 - 3\right) + \frac{K}{2}(J - 1)^2 \tag{S4}$$

Where μ is the shear modulus of the material and K is the volume modulus of the material. J is the deformation gradient determinant (i.e. Jacobi determinant), which represents the volume ratio of material elements before and after deformation. J is defined as formula S5.

$$J = \det(F) = \lambda_1 \lambda_2 \lambda_3 \tag{S5}$$

Considering the influence of the driving magnetic field on the deformation of the material, the strain energy density function of the NdFeB/Ecoflex magnetic response soft composite can be obtained by combining the formulas S3 and S4 as follows:

$$W = \frac{\mu}{2}\left(J^{-1.5} I_1 - 3\right) + \frac{K}{2}(J - 1)^2 + \frac{B_r^{'}}{\mu_0} e_m \cdot B^a \tag{S6}$$

The relationships between the Cauchy stress tensor **σ**, the strain energy density function W and the deformation gradient tensor F in the deformation process of the NdFeB/Ecoflex material model are shown in formula S7.

$$\sigma = \frac{1 \partial W}{J\, \partial F} \cdot F^T = \frac{\partial W}{\partial F} \cdot F^T \tag{S7}$$

By substituting formula S6 into formula S7, the Cauchy stress tensor in the process of magnetic drive deformation can be obtained, as shown in formula S8.

$$\sigma = \frac{1 \partial W}{J\, \partial F} \cdot F^T = \mu J^{-\frac{5}{3}}\left(F \cdot F^T - \frac{I_1}{3} I\right) + K(J - 1)I - \frac{1 B_r^{'}}{J \mu_0} B^a (F \cdot e_m) \tag{S8}$$

Formula S8 describes the stress-strain relationship of NdFeB/Ecoflex magnetically responsive soft composite during the magnetically driven deformation process, which can be integrated with the governing equations of the deformation process (the law of conservation of mass, the law of conservation of momentum and the law of conservation of moment of momentum) and the boundary conditions to establish the mathematical theoretical model of the magnetically driven deformation problem. The Abaqus mechanical simulation software can be used to solve the mathematical theoretical model, and then numerically simulate the deformation of NdFeB/Ecoflex magnetically responsive soft composite driven by an external magnetic field.

Note S2. The experimental process of obtaining the STR graphs of **Fig. S3-S5** and Success rate graph of **Fig. S6**.

Firstly, the MESR was placed horizontally on the experimental platform, and hydrogel balls with different diameters were placed in the second chamber of the MESR. Then, a 6-DOF machine hand control magnet was used to move along the preset trajectory to ensure the repeatability of the experiment (the manipulator photo is shown in **Fig. S8**). In the experiment, the magnet is controlled at the moving speed of the manipulator (20 mm/s), thus maximizing the transport speed of the MESR. Among them, each experiment in **Fig. S3-S5** was repeated three times, and each experiment in **Fig. S6** was repeated 25 times.